Supporting Information

Newbern *et al.* 10.1073/pnas.0805239105

SI Text

Transgenic Mice and Genotyping. Mice were housed and bred under standard conditions with food and water provided *ad libitum* and were maintained on a 12-h dark/light cycle. ERK1$^{-/-}$ mice possess a neo-insertion in exons 1 to 7 of the protein coding sequence, which includes the kinase domain (1). MEK1$^{fl/fl}$ mice possess a loxP flanked exon 3 whereas MEK2$^{-/-}$ mice contain a neo-insertion in exons 4 to 6, representing the kinase domain (2). B-Raf$^{fl/fl}$ mice were created by Dr. Alcino Silve (University of California, Los Angeles) and colleagues by inserting loxP sites around exon 9, and C-Raf$^{fl/fl}$ mice were a gift from Dr. Manuela Baccarini (University of Vienna) and possess a floxed exon 3 (3, 4). SRF$^{fl/fl}$ mice possess a floxed exon 1 (5). The Wnt1$^{Cre/wt}$ mouse was purchased from Jackson Laboratories. The mice used for this study had mixed genetic backgrounds.

Primers used for gene amplification are as follows: Wnt1:Cre, 5′-TTCGCAAGAACCTGATGGAC-3′ and 5′-CATTGCTGTCACTTGGTCGT-3′ amplify a 266-bp Cre allele; ERK1, 5′-AAGGTTAACATCCGGTCCAGCA-3′ and 5′-AAGCAAGGCTAAGCCGTACC-3′ amplify a 571-bp WT allele whereas 5′-AAGGTTAACATCCGGTCCAGCA-3′ and 5′-CATGCTCCAGACTGCCTTGG-3′ amplify a 250-bp knockout allele; ERK2, 5′-AGCCAACAATCCCAAACCTG-3′ and 5′-GGCTGCAACCATCTCACAAT-3′ amplify a 275-bp WT allele and a 350-bp floxed allele; MEK1, 5′- CAGAAGTTCCCACGACACTA-3′ and 5′-CTGAAGAGGAGTTTACGTCC-3′ and 5′-GTCTGTCACTTGTCTTCTGG-3′ amplify a WT and floxed allele; MEK2, 5′-CTGACCTTCCTGTAGGTG-3′ and 5′-ACTCACGGACATGTAGGA-3′ amplify a 293-bp WT allele whereas 5′-CTGACCTTCCTGTAGGTG-3′ and 5′-AGTCATAGCCGAATAGCCTC-3′ amplify a 450-bp knockout allele; B-Raf and C-Raf were genotyped as described previously (6); SRF, 5′-GGCACTGTCAGGGTGTCT-3′ and 5′-TGCTGGTTTGGCATCAACT-3′ yield a 515-bp band for the WT allele and a 350-bp band for the floxed allele.

Whole-Mount X-Gal Staining. Whole-mount X-Gal staining was performed using standard techniques. Briefly, fixed embryos were rinsed in PBS solution/2 mM $MgCl_2$ and incubated overnight in a PBS solution supplemented with 5 mM potassium ferrocyanide, 5 mM potassium ferricyanide, 2 mM $MgCl_2$, and 1 mg/ml X-Gal. After rinsing, embryos were postfixed with 4% paraformaldehyde and photographed.

1. Nekrasova T, *et al.* (2005) ERK1-deficient mice show normal T cell effector function and are highly susceptible to experimental autoimmune encephalomyelitis. *J Immunol* 175:2374–2380.
2. Belanger L-F, *et al.* (2003) Mek2 Is dispensable for mouse growth and development. *Mol Cell Biol* 23:4778–4787.
3. Jesenberger V, *et al.* (2001) Protective role of Raf-1 in Salmonella-induced macrophage apoptosis. *J Exp Med* 193:353–364.
4. Chen AP, *et al.* (2006) Forebrain-specific knockout of B-raf kinase leads to deficits in hippocampal long-term potentiation, learning, and memory. *J Neurosci Res* 83:28–38.
5. Ramanan N, *et al.* (2005) SRF mediates activity-induced gene expression and synaptic plasticity but not neuronal viability. *Nat Neurosci* 8:759–767.
6. Zhong J, *et al.* (2007) Raf kinase signaling functions in sensory neuron differentiation and axon growth in vivo. *Nat Neurosci* 10:598–607.

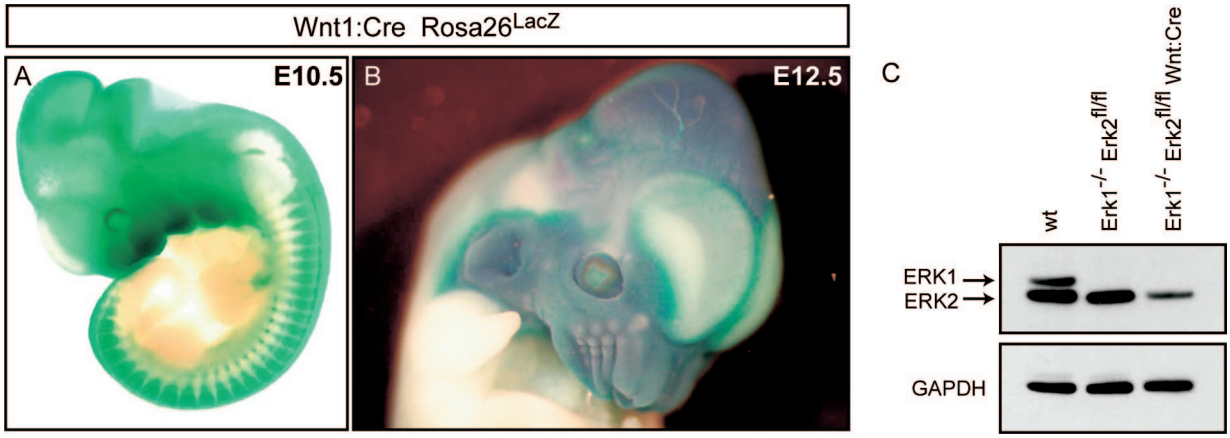

Fig. S1. Effective ablation of ERK1/2 signaling in neural crest-derived structures in ERK1$^{-/-}$ ERK2$^{fl/fl}$ Wnt1:Cre mice. Whole-mount LacZ staining of Wnt1:Cre × *Rosa26*$^{loxpSTOPloxp\text{-}LacZ}$ embryos reveals early recombination in mouse neural crest-derived structures at E10.5 (*A*) and 12.5 (*B*) in the pharyngeal arches, multiple craniofacial components, and peripheral nervous system. Protein lysates of dorsal root ganglia, a neural crest-derived structure, exhibit absence of ERK1 expression and significantly decreased ERK2 expression in E12.5 *ERK1*$^{-/-}$ *ERK2*$^{fl/fl}$ Wnt1:Cre mice (*C*).

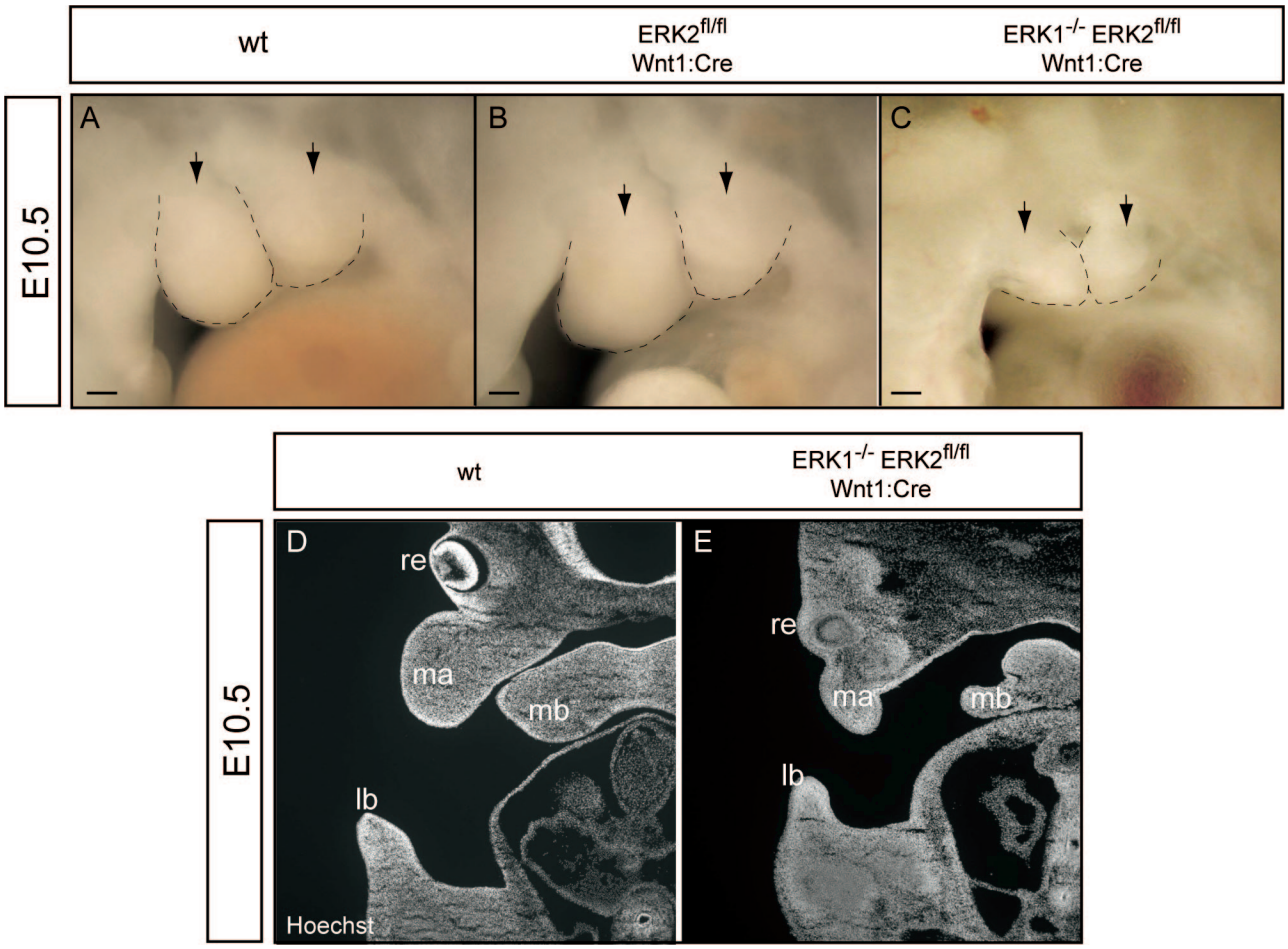

Fig. S2. Early defects in pharyngeal arch formation following the disruption of ERK1/2 signaling. Compared to WT controls (*A*), the size of the mandibular and maxillary components of pharyngeal arch 1 (arrows) is notably decreased in E10.5 *ERK1*$^{-/-}$ *ERK2*$^{fl/fl}$ Wnt1:Cre (*C*, $n = 3$ of 3) embryos, but not *ERK2*$^{fl/fl}$ Wnt1:Cre embryos (*B*) ($n = 7$). Cross-sections stained with a nuclear marker, Hoechst 33258, further illustrate the decrease in pharyngeal arch size in *ERK1*$^{-/-}$ *ERK2*$^{fl/fl}$ Wnt1:Cre embryos (*E*).

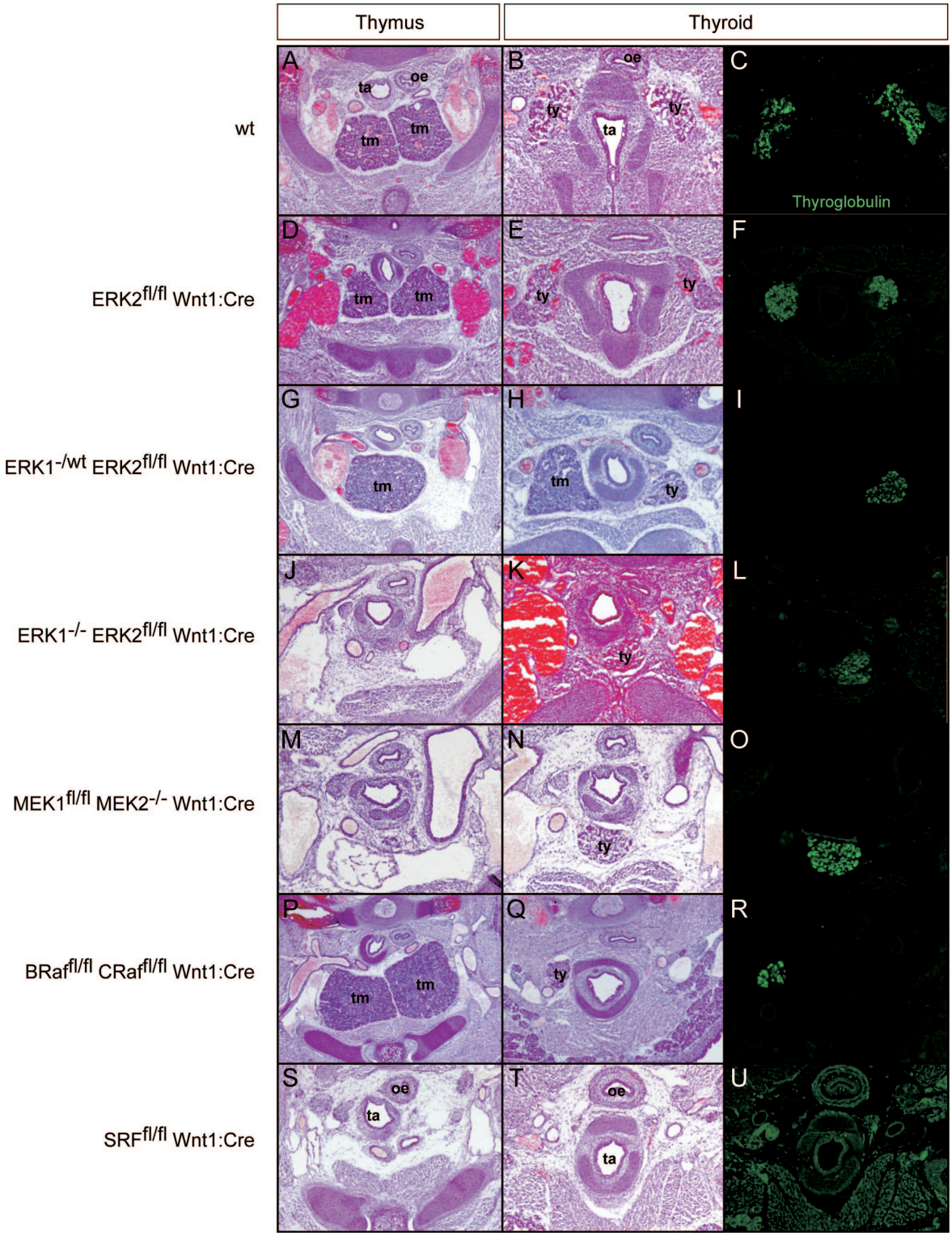

Fig. S3. Defects in thymic and thyroid development following the inactivation of upstream and downstream ERK1/2 signaling regulators. Compared to WT controls (*A–C*), cross-sections of E16.5 *ERK2*$^{fl/fl}$ Wnt1:Cre embryos did not exhibit significant morphological differences in thymus or thyroid histology (*D–F*). Thyroglobulin immunostaining was used to identify thyroid tissue. *ERK1*$^{-/wt}$ *ERK2*$^{fl/fl}$ Wnt1:Cre embryos exhibit a fused misplaced thymus (*G*) and misplaced thyroid (*H,I*), whereas *ERK1*$^{-/-}$ *ERK2*$^{fl/fl}$ Wnt1:Cre (*J–L*) and *MEK1*$^{fl/fl}$ *MEK2*$^{-/-}$ Wnt1:Cre (*M–O*) embryos exhibit thymic aplasia and thyroid misplacement. Thymus hypoplasia was variably penetrant in *B-Raf*$^{fl/fl}$ *C-Raf*$^{fl/fl}$ Wnt1:Cre embryos. Cross-sections of the E16.5 *B-Raf*$^{fl/fl}$ *C-Raf*$^{fl/fl}$ Wnt1:Cre embryo displayed in *P–R* did not exhibit an overt thymic defect, but thyroid hypoplasia and malpositioning were noted. SRF$^{fl/fl}$ Wnt1:Cre embryos exhibit aplasia of the thymus and thyroid (*S–U*). (oe = esophagus, ta = trachea, tm = thymus, ty = thyroid.)

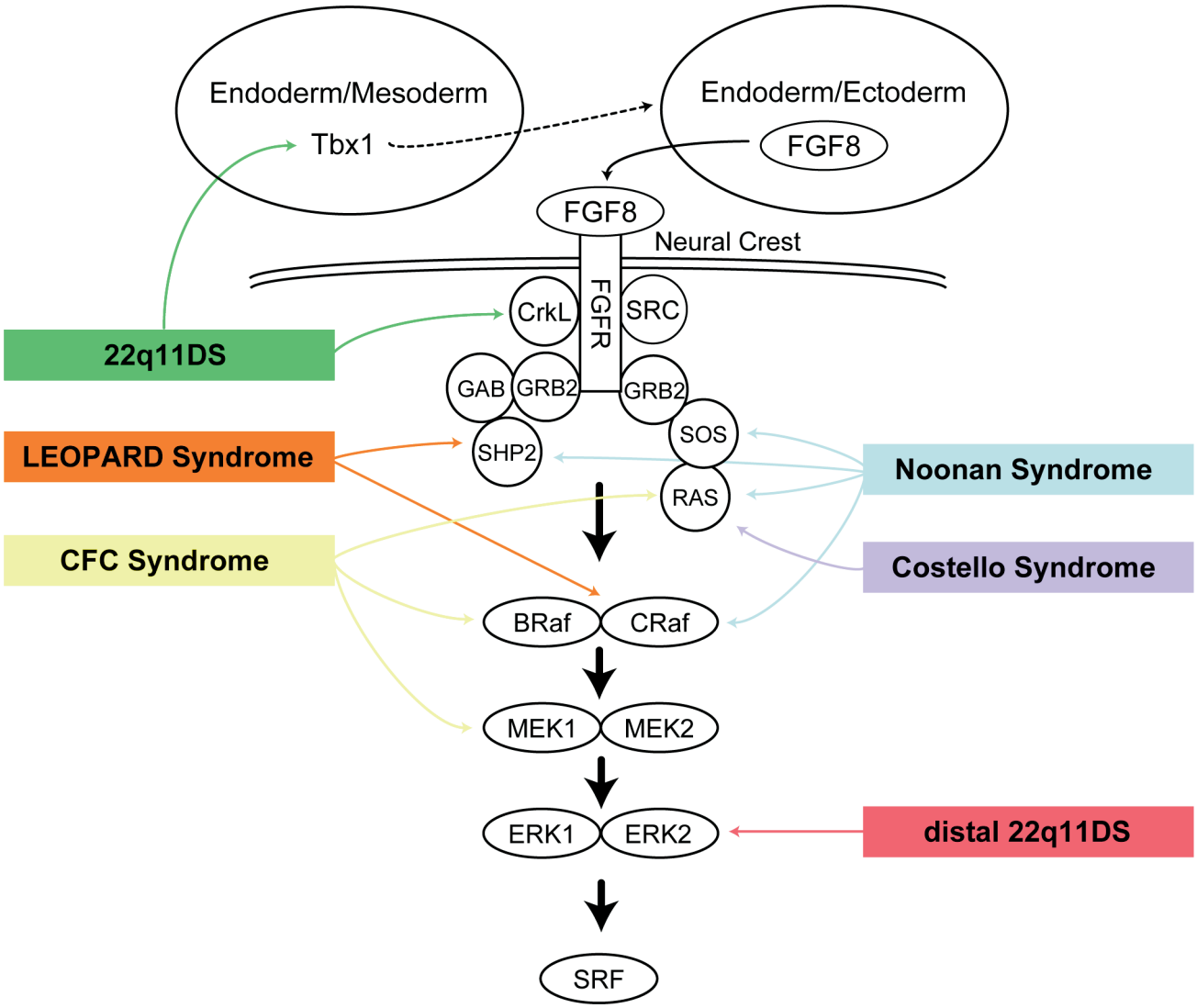

Fig. S4. Summary diagram of syndromes related to the Raf/MEK/ERK cascade and upstream regulators in human genetic disorders.